Proceedings of the 5th International Conference on Statistics: Theory and Applications (ICSTA'23)
Brunel University, London, United Kingdom – August 03-05, 2023
Paper No. 122
DOI: 10.11159/icsta23.122

Scalable Simulations of 3D Turbulence Fine Structure in Nanoflare Using a Novel Plasma Statistical Algorithm

Bojing Zhu[1,2,3*], Yan Li[1], Zhikuo Ma[1,3], Hui Yan[4], Ying Zhong[4], Wu Wang[5], Yufeng Guo[5], L.Zheng[6], David A Yuen[7]

[1] Yunnan Observatories, Chinese Academy of Sciences, Kunming, 650216, China (bjzhu@ynao.ac.cn)
[2] Centre for Astronomical Mega-Science, Chinese Academy of Sciences, Beijing, 100012, China
[3] School of Astronomy and Space Science & College of Earth and Planetary Sciences, University of Chinese Academy of Sciences, Beijing, 100049, China (cynosureorion@ucas.ac.cn)
[4] National Supercomputer center in Guangzhou, Sun Yat-sen University, Guangzhou, 510006, China
[5] Computer Network Information Centre, Chinese Academy of Sciences, Beijing, 10083, China
[6] National Supercomputer Centre in Chengdu, Sichuan, 610200, China
[7]Applied Physics and Applied Mathematics Department, Columbia University, New York, 10027, USA

Abstract **-**Based on algorithms of solving directly MHD partial differential equation algorithm (e.g., ATHENA [1], NIRVANA [2], ZEUS [3], FLASH [4], PIC [5-8], HPIC [9-11]), conventional simulation methods cannot attain the extreme range of scale for 3D turbulence fine-structure (Geometry and Physics) in flare-CME phenomena, especially for nanoflare heating problems. Here we present a parallel lattice Boltzmann algorithm based on plasma statistical physics, which allows us to reach even the relativistic regime necessary for modeling 3D turbulence fine-structure evolution. This innovative approach can simultaneously describe the continuous features of plasma at the macro-spatial-temporal scale, particle features of plasma at the micro-spatial-temporal scale, and particle features enforced by magnetic fields. However, the novel algorithm brings several challenges for fine-structure large-scale simulation, such as the gargantuan memory and storage requirements due to high dimensions and output data, and long simulation time, because each run takes a week. We propose optimization technologies for data access, communication, I/O, etc. These optimizations make it possible to achieve scalable and robust simulation (using up to 100,000 cores on the Tianhe-2 supercomputer) and the most extensive system ever run. For the first time, we can analyze the 3D turbulence fine structure by interacting with plasmas and magnetic fields in nanoflare.

Keywords**:** Novel parallel lattice Boltzmann algorithm, Tianhe-2 Supercomputer, 3D large spatial-temporal turbulence reconnection, Plasma statistical physics, Computational Statistics, Statistical methodology.

1. Introduction

Magnetic reconnection (MR) is recognized to be a key driver in controlling the behavior of the flare-CME phenomena, especially for nanoflare heating problems. Which involves complex multi-spatial-temporal scale and fully coupled magnetic field & plasma motion physical processes. Substantial research efforts have shown that many kinetic scale fractal and turbulence magnetic structures [12-21].

We define these typical 3D continuous kinetic-dynamic-hydro (KDH) fully coupled MR on the solar-terrestrial space environment as 3D large spatial-temporal scale turbulent MR (3D LTSTMR) [22-24]. There are still many uncertainties (e.g., flare heating, wave-particle interaction acceleration) due to the limitation of current observation technologies and the incompleteness of the present theoretical system. As an independent way from theory and observations, numerical simulation provides an essential means for exploring the above phenomena. However, the conventional magnetohydrodynamics (MHD) simulation method (e.g., [1-11]) applied for simulating the discrete process by directly solving nonlinear coupled MHD partial differential equations (PDEs), is not able to comprehensively describe the following principal properties of LTSTMR at the same time:

1. Small-scale kinetic particle characteristics.
2. Large macro-scale dynamic flow characteristics.
3. The particles and flows controlled by magnetic fields fluctuation-induced self-generating-organization (MF-ISGO), the plasma turbulence-induced self-feeding-sustaining (PT-ISFS), and the interaction of turbulence between MF-ISGO and PT-ISFS).

Some algorithms (e.g., ATHENA [1], NIRVANA [2], ZEUS [3], FLASH [4]) are suitable for investigating plasma dynamics with large macro-scale properties, some algorithms (e.g., PIC [5-8], testing particles [9-11]) are suitable for investigating plasma properties with micro-scale properties. The significant challenges that need to be solved in the numerical simulation are as follows:

1. In the continuous KDH fully coupled LTSTMR simulation domain, the scales of x, y, and z are on the order of 10E10 ~10E11, 10E8 ~10E9 and 10E7~10E8, respectively; in other words, the geometric simulation domain is a box in which the x-coordinate spans from 0.2 m to 1000,000 km, the y-coordinate spans from 0.2 m to 500,000 km, and the z-coordinate spans from 0.2 m to 100,000 km, respectively. The evolution time-scale is of the order of 10E10 ~10E11, ranging from 10E-5s to 10E5s; the temperature, density, ionization, magnetic strength, electron energy, and proton energy scales range respectively from 3,000 K to 1000,000 K, 10E27 m^{-3} to 10E15 m^{-3}, 10E(-6) to 10 G to 1,000G, KeV to MeV, and KeV to GeV (>100MeV, γ-ray emission), respectively. The number of generalized hyper-singular terms in the distribution functions is larger and more complicated than the conventional MHD models in realistically turbulent plasma. All distribution functions (DFs) must meet the self-consistent conditions in the evolution of the entire domain.
2. To describe the particles' behaviours inside the present model for each type of species, a set of configuration variables and parameters need to be defined in the whole simulation domain (ideal MHD region, hydro scale), the ion diffusion region (non-ideal ion MHD (IMHD); dynamic scale), and the electron diffusion region (non-ideal electron MHD (EMHD); kinetic scale) respectively.
3. To describe nonlinear and continuous KDH fully coupled evolution in the physical picture, we must ensure that enough hyper-singular terms are included in the DF within the sensitive physical system. Moreover, the hyper-singular terms significantly impact the stability of the numerical simulation system, which is one of the algorithm's significant sources of numerical instability.
4. The continuous fully coupled 3D LTSTMR simulations have high requirements over the memory, processing unit (central processing unit, CPU), data communication, and serial/parallel I/O controllers (IOC). Recently, some researchers put forward the lattice Boltzmann method (LBM) in plasma simulation, which differs from the conventional way of directly solving the PDEs algorithm [25-32]. At the same time, the essential core of statistical mechanics in this methodology brings the advantages of a more natural description of plasma properties and the disadvantages of a tremendous computation cost. This results in the LBM requiring more computing resources (RAM, CPU, IOC, and so on) than the traditional method of directly solving PDEs [1-11]. There has been unprecedented development of supercomputing platforms, making it possible to realize highly large-scale LBM.

In this paper, we have developed a novel massively parallel LBM algorithm based on plasma statistical physics. This accomplishment allows us to get into the relativistic regime, which is essential for understanding the LTSTMR. Our innovative and daring approach can simultaneously describe the continuous features of plasma at the macro-spatial-temporal scale and particle features of plasma at the micro-Spatial-temporal scale of MR, which provides spherical geometry with both adequate spatial and temporal resolution. We then ran many cases, over 1000 of them, and used up to around 140 million CPU core hours on the Tianhe-2 Supercomputer at National Supercomputer Canter in Guangzhou (NSCC-GZ). Our heroic effort, together with the present algorithm, makes it possible, for the first time, to analyze the fully coupled self-generated turbulence by B and U collective interaction from the physical model directly. In Section 2.1, we introduced the set of equations for plasma statistical simulation methods, in which partial distributions are solved on a discrete lattice, in contrast to conventional MHD methods, which involve a numerical solution to PDE. In section 2.2, we present the evolution equations for the LBM DFs. In section 2.3, we introduce the framework-flowchart implementation of the parallel processing and the details of our parallel code design. We applied it to analyze large-scale 3D turbulence generated by plasmas within a magnetic field for the first time in section 3. Finally, we summarized the advantage of the present lattice Boltzmann algorithm. We introduced its possible applications in areas other than the flare-CME phenomena, such as the Sun-Earth system or the geo-dynamo problem in the planetary cores, which is very different from the usual spherical harmonic expansion.

2. Methodology

2.1 Basic equations

The governing formulations of the plasma statistical algorithm and magnetic induction equation for resistive relativistic MHD can be written as [22-24,33-34],

$$\frac{\partial f^{\alpha}}{\partial t}+\frac{1}{\varepsilon^{\alpha}}\boldsymbol{U}^{\alpha}\cdot\nabla f^{\alpha}+\left(\frac{1}{\varepsilon^{\alpha}}\boldsymbol{E}+(\delta^{\alpha})^{2}\boldsymbol{U}^{\alpha}\times\boldsymbol{B}\right)\cdot\frac{\partial f^{\alpha}}{\partial \boldsymbol{p}^{\alpha}}=-(\varepsilon^{\alpha})^{2}\nabla_{\boldsymbol{p}^{\alpha}}\cdot\left(\nabla_{\boldsymbol{p}^{\alpha}}f^{\alpha}+\boldsymbol{U}^{\alpha}f^{\alpha}\right) \tag{1}$$

Based on the mean-field theory, the relativistic U, B, and E are decomposed into their average and fluctuation components, which vary depending on the hydro-dynamic and kinetic scales. Then, the full-blown magnetic induction in the whole simulation domain and self-generated magnetic fields can be written as Eq. (2-3) [22-24, 35-37] and Eq. (4) [38,39], respectively.

$$\frac{\partial \bar{\boldsymbol{B}}}{\partial t}=\nabla\times(\bar{\boldsymbol{U}}\times\bar{\boldsymbol{B}})-\nabla\times(\hat{\alpha}\bar{\boldsymbol{B}})+\hat{\beta}\nabla^{2}\bar{\boldsymbol{B}}+\eta_{s}\nabla^{2}\bar{\boldsymbol{B}} \tag{2}$$

$$\frac{\partial \tilde{\boldsymbol{B}}}{\partial t}=\nabla\times\left(\bar{\boldsymbol{U}}\times\tilde{\boldsymbol{B}}\right)+\nabla\times\left(\tilde{\boldsymbol{U}}\times\bar{\boldsymbol{B}}\right)+\nabla\times\left(\tilde{\boldsymbol{U}}\times\tilde{\boldsymbol{B}}\right)-\nabla\times(\hat{\alpha}\bar{\boldsymbol{B}})+\hat{\beta}\nabla^{2}\bar{\boldsymbol{B}}+\eta_{s}\nabla^{2}\tilde{\boldsymbol{B}} \tag{3}$$

$$\frac{\partial \boldsymbol{B}}{\partial t}=\nabla\times\left\{\begin{array}{l}\underset{(a)}{\frac{m_e}{e}\frac{\partial \boldsymbol{U}_e}{\partial t}}+\underset{(b)}{\frac{m_e}{e}(\boldsymbol{U}_e\nabla)\boldsymbol{U}_e}+\underset{(c)}{\frac{1}{en_e}\nabla P_e}+\underset{(d)}{\frac{1}{en_e}\nabla\boldsymbol{\pi_e}}+\underset{(e)}{\frac{m_e}{e}\langle\xi\cdot\nabla\cdot\xi\rangle}+\underset{(f)}{\boldsymbol{U}_e\times\boldsymbol{B}}-\underset{(g)}{\alpha_{\parallel}(\boldsymbol{J}\cdot\boldsymbol{b})\boldsymbol{b}}- \\ \underset{(h)}{\alpha_{\perp}\boldsymbol{b}\times(\boldsymbol{J}\times\boldsymbol{b})}+\underset{(i)}{\alpha_{\Lambda}(\boldsymbol{b}\times\boldsymbol{J})}+\underset{(j)}{\frac{\beta_{\parallel}}{e}(\nabla T_e\cdot\boldsymbol{b})\boldsymbol{b}}+\underset{(k)}{\frac{\beta_{\perp}}{e}\boldsymbol{b}\times(\nabla T_e\times\boldsymbol{b})}+\underset{(l)}{\frac{\beta_{\Lambda}}{e}(\boldsymbol{b}\times\nabla T_e)}+\underset{(m)}{\left\langle\xi\times\tilde{\boldsymbol{B}}\right\rangle}\end{array}\right\} \tag{4}$$

The interaction between the magnetic field and plasma motion is translated into the interaction between different lattice grids in the KDH model. The pseudo-Larmor radius and pseudo gyroperiod of charged particles are defined by using the fractal index and adaptive lattice grid refinement, which significantly improved the computation efficiency compared with a traditional algorithm [1-11]. In our innovative algorithm, a set of equations for non-ideal MHD are solved in phase space which is of higher dimension (six) than the usual three-dimensional method, and the numerical dispersion error is suppressed.

2.2 Distribution Function (DF)

In our model, the magnetic field, the electric field, and the electromagnetic field in the diffusion region of the resistive relativistic LTSTMR are defined as the virtual magnetic flow composed of pseudo-magnetic particles, the virtual electric flow composed of pseudo-electric particles, and the virtual electromagnetic flow composed of pseudo-electromagnetic particles, respectively. The virtual flow (virtual magnetic flow, virtual electric flow, and virtual electromagnetic flow) and actual flow (ion flow, electron flow, and neutral flow) are respectively defined using DB3Q7, DE3Q13, De3Q19, Di3Q19, and Dn3Q27 lattice grids. The interactions and/or collisions between real particles (charged particle-to-charged particle, charged particle-to-neutral particle, neutral particle-to-neutral particle) are accurately described by these lattice grids [22-24, 35-37] (Figure 1). The interactions between the fields (magnetic, electric, and electromagnetic) and the particles (neutral and charged particles) transformed into interactions between pseudo-particles in virtual flow and real particles in real fluid flow in the present algorithm system. Therefore, one outstanding issue is the interaction between pseudo and real particles in the regime where resistive relativistic MHD diffusion dominates. In this 7-dimensional spatial-temporal space, the geometry space (geometry simulation domain) and physical space (motion turbulence, field fluctuation, and the interaction between them) are classified into regular cubic lattice grids. Each lattice grid has x_i extended vectors that link the grid with its neighbours. Each extended vector is associated with a DF. We do not know that the computational domain is spherical because we have started with a cube and have cut truncated the eight corners to approximate a sphere. Then, we can combine all the discretized equilibrium DF, MF-ISGO, PT-ISFS, and interaction of turbulence between MF-ISGO and PT-ISFS in the resistive relativistic MHD can be translated into the interactions and collisions of the extended particles by the following framework-flowchart and its implementation.

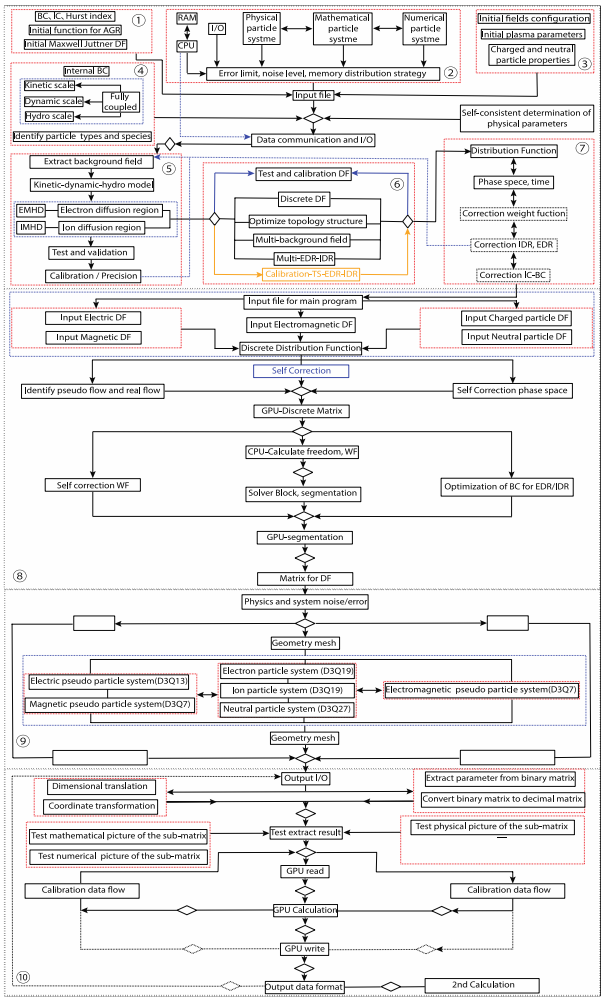

Figure 1: Schematic of the flowchart and implementation for the input model (Workflow A), the discrete distribution function (workflow B), evolution and I/O (workflow C), and output analysis (workflow D). Pseudo-code diagram for the flow chart link: https://pan.cstcloud.cn/s/4XBboTmcSkI.

2.3 Flowchart of the massively parallel program

We develop a robust novel model to solve MR problems in realistically turbulent plasma. LTSTMR has many difficulties in physical, mathematical, and numerical modeling. This algorithm program consists of three parts (input file preparation, computing, and output data analysis), written in multiple languages (C, FORTRAN, PYTHON, IDL, and Tecplot scripts). The pre-process, post-process, and visualization are based on a GPU-CPU heterogeneous computing system, which has a significantly different architecture and program skeleton pink from the CPU isomorphic computing system. A discrete CPU-GPU system provides high performance but has the disadvantage of slow communication between the GPU cores and CPU cores. In the large-scale simulation, we divide computing and communication into two separate processes; the CPU handles the HPC computing tasks, while the GPU handles the post and communication processes. The present algorithm is costly regarding computational resources and memory, even the adaptive lattice grid refinement (GALGR and PALGR). Compared to the conventional MHD algorithms, this dramatically improves computational efficiency. The pseudo-Larmor radius and pseudo-cyclotron time of the charged particles are defined and applied by the fractal index in the algorithm. The high costs come from the following three factors: 1) The self-consistency between the geometric adaptive lattice grid refinement (GALGR) and physical adaptive lattice grid refinement (PALGR, DB3Q7, DE3Q13, De3Q19, Di3Q19, Dn3Q27). Improper setup causes physical, numerical and system errors that terminate the main program. 2) The self-consistency between the numerically implemented matrices size (collision and interaction between different size lattice grids) and main memory.

Improper setup results in reduced computational efficiency and leads to transient node overload. 3) The noise (error) due to the improper setup of initial conditions leads to simultaneous transient overload of all the nodes, which can cause the system to fail.

Now we display our novel massively parallel LB algorithm by showing the flowchart framework of pseudo code and how to implement this to demonstrate how this algorithm can successfully solve the 3D LTSTMR. We set down the basic definitions of the lines, arrows, special symbols, and texts used in the flowcharts and pseudo codes in the flowcharts and pseudo codes (Figure 1).

1. Geometry & physics input: The D(i)XQY (X and Y denote the dimensionality and the number of discrete physical variables; DB3Q7, DE3Q13, DEM3Q13, De3Q19, Di3Q19, Dn3Q27), the DF are defined in the simulation domain.

2. Error limit, noise level, and memory: To maintain the load stability (CPU and RAM loads), we define different error limits and noise level modes at different temporal-spatial scales. A framework for predicting the computational resource consumption (CRC) of CPU (CRC|_CPU) and memory (CRC|_RAM) is designed in the algorithm. When the two predicted values (CRC|_CPU, CRC|_RAM) are inconsistent, the maximal value is used as a parameter in the input file. Another method to reduce the CPU and RAM loads is to control the number of super-particles in each DXQY model during the evolution.

3. Normalization and self-consistent determination: Normalization is essential in implementing the algorithm, especially for studying self-consistent determination in the relaxation of interaction between particles. The input setup section transforms all the input variables and parameters into dimensionless values. The self-consistent determination for the initial fields and the plasma parameters in the ideal and non-ideal MHD (IMHD and EMHD) simulation domain is performed by applying Gauss's law of magnetism and the continuity equation.

4. Identify particle types, species, and initial boundary condition: There are several types and species of particles throughout the simulation box; to make all the streaming and collisions (direct and indirect) can add to all the different particles of the system, the interactions between particles on the background (BG), current sheet (CS), and on the boundaries of the BG and CS have been defined.

5. Discretization of DF: The most natural representation of the joint discrete DFs is as six (zeta=1 ~ 3, B, E, and EM) 8 × 28 matrices of 8×28 independent components for each species (iota = 1,2,3...). The eight dimensions are based on the arrays. The CPU matrices store the discrete DF for subsequent calculations in the main program. The GPU matrices, created according to the structures of the 8x28 matrices, are accountable for analysing the output data. The MHD plasma is composed of mixed particles (iota=1, Hydrogen; nu < 0, ionized plasma) and is taken as an example for discretizing the DF and introduced as follows (Figure 1). 1) Building the discrete DF matrices from GPU cores, where each component value of the given matrices is a function of eight independent variables: 2). Converting the six DF matrices into a general discrete DF matrix, identifying the virtual and the real flow, and finishing the self-correction test in the phase space using Gauss's law of magnetism and the continuity equation; 3) Decomposing the algebraic expression of the discrete DF, determining the relationship between the DF_8×99 and the ionization parameter; 4) Converting DF_8×99 into an array DF__GPU in the GPU cores. The algorithm can utilize more resources on each GPU processor than on a CPU processor, which can store the discrete distribution function matrices on the continuous KDH fully coupled temporal-spatial scale; 5). Establishing a new array architecture based on DF_GPU, then saving it to investigate the output data created in Evolution and post process.

6. Evolution

This part of the computation consumes most computational resources. We create different arrays to save all the physical parameters and then use these arrays to monitor the CPU, memory, and communication loads at every simulation time step.

3. Applications

To verify the reliability of the present algorithm, we applied the developed code to investigate the LTSTMR. Here the complex 3D turbulence features in the MF-ISGO, the PT-ISFS, and the interaction of turbulence between MF-ISGO and PT-ISFS in the continuous KDH fully coupled LTSTMR were simulated for the first time. The followings are some basic parameters used in these simulations. The proton to electron mass ratio is assumed to be m_i/m_e=1836, and the electron CSs with peak density n_0 superimposed on a uniform BG density n_b=0.05×n_0 is set up in 3D (x,y,z) space =16000×32000×16000 lattice gird points. The total number of SPs is 8000×16000×8000×2$\hat{n}$, where $\hat{n} > 8$ and depends on the number density of the BG. The initial magnetic configuration is normalized, and the simulation results are presented in normalized units. Both force-free MR (including resistive tearing model, ideal MHD kink mode) and forced MR evolution manner are considered. From the simulation results, we can summarize:

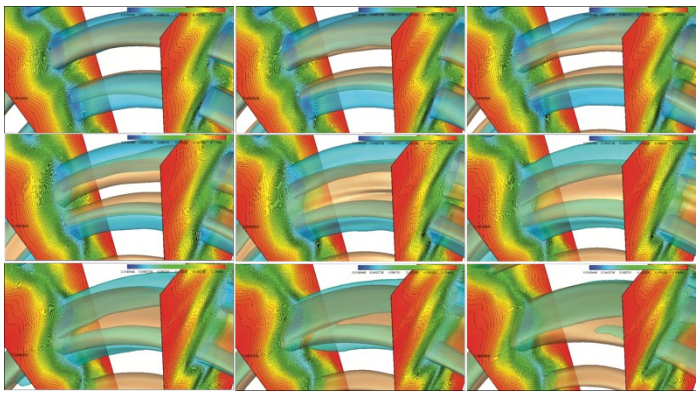

Figure 2: Interaction between twisting magnetic vortex flux tube (yellow) and twisting plasma fluid vortex flux tube (blue) in the self-generated turbulence evolution in B and U decoupled beyond ideal MHD diffusion region from $6522800\omega_{ci}^{-1}$ to $6602800\omega_{ci}^{-1}$. Animation online file http://ddl.escience.cn/f/UIUF.

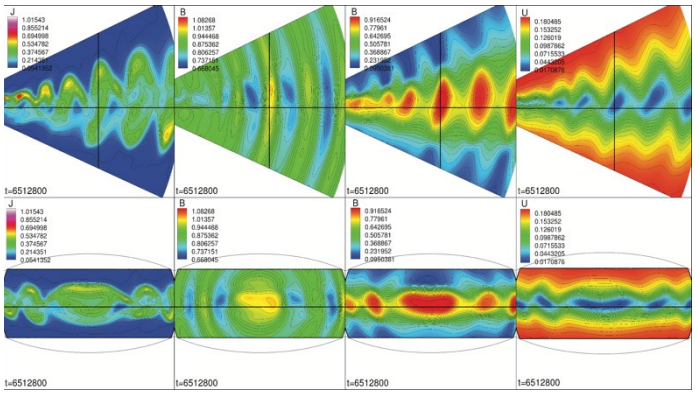

Figure 3: Magnetic field vortex shedding-driven by plasma fluid vortex flux tube vs. Plasma fluid field vortex shedding -driven by magnetic vortex flux tube from 6522800 $\omega_{ci}^{-1}$to 6602800 ω_{ci}^{-1} .Animation online file https://pan.cstcloud.cn/s/ikIgLHMFTaE.

1. The self-generated turbulence by the magnetic field and plasma motion collective interaction includes two fully coupled processes of (1) fluid vortex-induced MR and (2) MR-induced fluid vortex. The Biermann Battery Term and α-effect can not only generate magnetic fields, but can serve them to trigger MR, and the Spitzer resistance and turbulence resistance can not only generate magnetic eddies but can help to trigger fluid turbulence.

2. These interaction leads to vortex splitting and phase separating instabilities, and there are four species instabilities that coexist in the evolution process: 1) Vortex separation interface instabilities. 2) Magnetic fluctuation-induced self-generating-organization instabilities. 3) Plasma turbulence-induced self-feeding-sustaining instabilities. 4) Vortex shedding instabilities (Figures 2 and 3). All the simulation results agree well with the latest observational data [48-49] and theories [40-47].

4. Conclusions

We have developed and exploited a novel massively parallel lattice Boltzmann algorithm, based on plasma statistical physics [40-45] to investigate large-scale turbulence generated by involving plasmas and magnetic field in LTSTMR in Solar-Earth system. First, we introduced in detail the design and implementation of the novel LBM algorithm, which models number densities on a discrete lattice. We tested the mathematical algorithm's correction, reliability, stability, and efficiency [22-24,27]. We can explain the reason for the suitability of this innovative and daring approach to be able to simultaneously describe the continuous feature at macro-temporal-spatial and particle feature at micro-temporal-spatial MR, which are

modeled in spherical geometry with both enough spatial and accurate temporal resolution. Second, we have shown that the proposed optimization algorithms have improved the developed program's performance, enabling scalable and robust runs over the Tianhe-2 system. Third, we used our algorithm to simulate the basic features of the turbulence in the MF-ISGO, the turbulence in the PT-ISFS, and the interaction of turbulence between MF-ISGO and PT-ISFS in the continuous KDH fully coupled 3D LTSTMR for the first time. All the simulation results agree well with the latest observational data [48-49] and theories [40-47]. In general, a major effort together with the present algorithm make it possible for the first time ever to analyze the fully coupled self-generated turbulence by plasmas and magnetic collective interaction from the physical model directly. Our approach surpasses previous numerical efforts such as those used in other MHD equations because we have (1) a more complete set of equations in MHD and plasma dynamics, (2) a superior discretization scheme using LBM, and (3) a very powerful supercomputer, Tianhe-2. With the advantage of the present algorithm, we also see possible applications in fields other than flare-CME phenomena, such as the Sun-Earth system or the Planetary interior dynamo problem, using a method different from the usual spherical harmonic expansion.

Code and data availability statement

All the code and original data supporting this study's findings will be available from the corresponding author through NSCC-GZ, NSCC-CAS, and CAS Cloud, without undue reservation.

Acknowledgment

Based on the NSFC Fund 042274216 (PI: B.J.Zhu), the Specialized Research Fund for State Key Laboratories (PI: B.J. Zhu), and the NSFC Fund 042274216 (PI: B.J.Zhu), the HIECO Fund 202202014479 (A) (PI: B.J.Zhu), the super computation of the NSFC-Guangdong joint fund U1501501 (second phase), the NSF Fund EAR-1918126 (PI: Renata Wentzcovitch, David A Yuen), the US Department of Energy award (DESC0019759), the National Key RD Program of China (2022YFF0503800), the NSFC Key Fund 11933009, and the NSFC Key Joint Fund U1911204.

Thanks, Prof.Y.T.Lu, Prof. Y.F.Du, Dr. J.K.Chen, Dr. W.Wan, Dr. H.Z.Lu, and other members of NSCC-GZ for supercomputer services. Thanks to Dr.L.P.Liu, Prof.X.B.Chi, and other CNIC of CAS for HPC services. Thanks to Dr. Hui Li, Dr. Shengtai Li, Dr. Fan Guo, Dr. Xiaocan Li, and other members of the T2 and T5 Division of Los Alamos National Laboratory for helpful discussion on vortex/turbulence role in particles accelerations and magnetic energy translation.Thanks to Prof.Y.C.Ye of the National University of Defense Technology for supercomputer services. Thanks to Dr.C.Wang of NSCC-TJ for supercomputer services. Thanks to Dr. W. Tian, Dr. W.Yan, Dr.Y.W.Shi, and other members of PARATERA for supercomputer services and helpful discussion on the optimization of RHPIC-LBM2. Thanks to Prof.Y.L.Shi, Prof.Y.Z.Zhou and Prof. H.H. Cheng of the University of Chinese Academy of Sciences for helpful discussion on LBM and simulations parts. Thanks to Prof. K. Fujimoto of Beihang University for a proper debate on adaptive mesh refinement (AMR), grid convergence index (GCI), and statistical reliabilities technologies of PIC methodologies. Thanks to Prof. J. Lin of Yunnan Observatories of CAS for the helpful discussion on the concepts of sizeable temporal-spatial turbulence magnetic reconnection in the solar atmosphere. Thanks to Prof. Y.Bi of Yunnan Observatories of CAS for discussing nanoflare's observational and theoretical analysis.Thanks to Dr. W. Jin of Kunming Radio Wave Observatory of CRIRP for the valuable discussion on observations of space physics. Thanks to Prof. H.B.Li and Prof.Hsiang.H.Wang of the Department of Physics of The Chinese University of Hong Kong for helpful discussion on turbulence and B field. Thanks to Prof. J.S. Zhao of Purple Mountain Observatory of CAS for the valuable discussion on particle acceleration over the complete range of accelerated particles observed in the solar atmosphere. Thanks to Prof. D.J. Wu of Purple Mountain Observatory of CAS for the helpful discussion on the nature of turbulence. Thanks to Prof.J.S.He of the School of Earth and Space Sciences, Peking University, for useful discussion on the dispersion and dissipation in magnetic reconnection turbulences. Thanks to Dr. D.Verscharen of the Department of Space and Climate Physics, University College London, discusses the simulation methodologies in turbulent MR.

References

[1] J.M. Stone, T.A. Gardiner, P. Teuben, et~al. Astrophys. J, 178,137-177,2008.
[2] U. Ziegler, Comput Phys Commun, 179,4,2008.
[3] D.A. Clarke, Astrophys. J, 187,119-134,2010.
[4] B. Fryxell,K. Olson, P. Ricker, et~al. Astrophys. J, 131,1,2000.

[5] T.A. Nakamura, H. Hasegawa, W. Daughton, et~al. Nat. Phys,8,1582, 2017.
[6] T.Nakamura, W. Daughton, FUS034,178,137-177,2017.
[7] K. Fujimoto, J. Comput. Phys, 230,23,2011.
[8] K. Fujimoto, Geophys. Res. Lett, 43,20,2016.
[9] K. Nakwana, R. Keppens, G. Lapenta, J. Phys. Conf. Ser,1031,012019,2018.
[10] B. Ripperda, O. Porth, C. Xia,R. Keppens, Mon. Notice. Royal. Astron. Soc,467,3279,2017.
[11] B.Ripperda, O. Porth, C. Xia, R.Keppens, Mon. Notice. Royal. Astron. Soc,471,3465,2017.
[12] T.G. Forbes, Geophys. Astrophys. Fluid. Dyn, 62, 1-4, 1991.
[13] J.S. He, E. Marsch, C.Y. Tu, H. Tian, Astrophys. J. Lett, 705,2,2009.
[14] D.J. Wu, Science Press, 2, 200,2010.
[15] D.I. Pontindi, Adv. Space. Res, 47, 9,2011.
[16] H.T. Ji, W. Daughton, Phys Plasmas, 18,111207,2011.
[17] H.S.Fu, Y.V. Khotyaintsev, A.Vaivads, A.Retino, M. Andre, Nat. Phys, 9,7, 2013.
[18] Q.Q. Shi, Q.G. Zong, S.Y. Fu, et~al. Nat.Commun, 4,1466, 2013.
[19] J. Lin, N.A. Murphy, C.C. Shen, et~al. Space. Sci. Rev,194,1-4, 2015.
[20] R.S. Wang, Q.M. Lu, R.Nakamura, et~al. Nat. Phys,12,3, 2016.
[21] R.B. Torbert, J.L. Burch, T.D. Phan, et~al. Science, 362,6421,2018.
[22] B.J. Zhu, H.Yan,D.A. Yuen, Y.L. Shi, Earth. Planetary. Phys, 2019.
[23] B.J. Zhu, H.Yan, Y. Zhong, et~al. Appl Math Model, 78, 932, 2020.
[24] B.J. Zhu, H. Yan, Y. Zhong, et~al. Appl Math Model, 78, 968,2020.
[25] J.D. Mendoza, Phys. Rev. E, 77,2,2008.
[26] P.J. Dellar, J. Comput. Phys,237,15,2011.
[27] H.H. Cheng, Y.C. Qiao,C. Liu, et~al. Appl. Math. Model, 36,5,2011.
[28] P. Romatschke, F. Mohsen,M. Mendoza,S. Succi, Phys. Rev. C,84,3,2011.
[29] F. Mohsen, M.Mendoza, S. Succi,H.J. Herrmann, Phys. Rev. E,92,2,2015.
[30] L. Ottolenghi, P. Prestininzi,A. Mendoza, et~al. Eur. J. Mech. B/Fluids,67,1,2018.
[31] D. Place,P. Mora, Phys. Earth. Planet. In,150,2,1998.
[32] P. Mora,D.A.Yuen, Phys. Earth. Planet. In,275,1,2018.
[33] A. Brizard,A.A.Chan, Phys. Plasmas, 6,12,1999.
[34] M. Mendoza,B. Boghosian,H.J. Herrmann,S. Succi, Phys. Rev. Lett, 105, 055101,2010.
[35] D. Biskamp, H. Welter, Phys. Rev. Lett, 44, 16,1980.
[36] D. Biskamp, Astrophys. Space. Sci, 242,1-2,1996.
[37] D. Biskamp, Cambridge.Univer.Press, 3. 2000.
[38] M. Sherlock, Phys.Rev.Lett, 104. 20,2010.
[39] M.G. Hanies, Can. J.Phys, 64. 8,1986.
[40] U. Frisch,A. Pouquet, J. Leorat, A. Mazure, J.Fluid.Mech, 68.4,1975.
[41] D. Eyfe,J. Montgomery, J, J.Plasma. Phys, 16.2,1976.
[42] T. Stribling,W.H. Matthaeus, Phys. Fluids. B, 1979,2,1990.
[43] R. Jordan,Z.Yoshida, N. Ito, Physica, D, 114,3-4,1998.
[44] S.Servidio,W.H. Matthaeus, V. Carbone, Phys. Plasmas, 15,4,2008.
[45] S.Friedli,Y. Velenik, Cambridge Univ Press, 2017,2,2017.
[46] V.M. Nakariakov,M.J. Aschwanden,T.V. Doorsselaere, Astron. Astrophys, 502, 2,2009.
[47] M. Gruszecki,V.M. Nakariakov, T.V. Doorsselaere, Phys. Rev. Lett., 105, 055004,2010.
[48] T. Samanta,H. Tian, V.M. Nakariakov, Phys. Rev. Lett., 123, 035102,2019.
[49] P. Syntelis,P. Antolin, Astrophys. J. Lett, 8841,1,2019.